Published in final edited form as:
Dev Dyn. 2011 March ; 240(3): 704–711. doi:10.1002/dvdy.22557.

Nodal-mediated epigenesis requires dynamin-mediated endocytosis

Robin P. Ertl[1], **Anthony J. Robertson**[1], **Diane Saunders**, and **James A. Coffman**[2]
Mount Desert Island Biological Laboratory, PO Box 35/Old Bar Harbor Road, Salisbury Cove, ME 04672

Abstract

Nodal proteins are diffusible morphogens that drive pattern formation via short-range feedback activation coupled to long-range Lefty-mediated inhibition. In the sea urchin embryo, specification of the secondary (oral-aboral) axis occurs via zygotic expression of *nodal*, which is localized to the prospective oral ectoderm at early blastula stage. In mid-blastula stage embryos treated with low micromolar nickel or zinc, *nodal* expression expands progressively beyond the confines of this localized domain to encompass the entire equatorial circumference of the embryo, producing radialized embryos lacking an oral-aboral axis. RNAseq analysis of embryos treated with nickel, zinc or cadmium (which does not radialize embryos) showed that several genes involved in endocytosis were similarly perturbed by nickel and zinc but not cadmium. Inhibiting dynamin, a GTPase required for receptor-mediated endocytosis, phenocopies the effects of nickel and zinc, suggesting that dynamin-mediated endocytosis is required as a sink to limit the range of Nodal signaling.

INTRODUCTION

Nodal proteins are TGFβ-family signaling ligands that mediate epigenetic symmetry breaking processes in animal development, including mesoderm induction in vertebrates, axial patterning of neuroectoderm in vertebrates and echinoderms, and left-right axis specification in chordates, echinoderms, and gastropods (Schier and Shen, 2000; Duboc et al., 2004; Chea et al., 2005; Duboc et al., 2005; Lupo et al., 2006; Shen, 2007; Grande and Patel, 2009). In deuterostomes *nodal* is part of a feedback circuit wherein autocrine and paracrine Nodal signaling locally activates the *nodal* gene, as well as expression of its competitive inhibitor Lefty, which is more diffusible than Nodal and hence restricts the domain of *nodal* activity (Juan and Hamada, 2001; Chen and Schier, 2002; Duboc et al., 2008). Thus, *nodal* and *lefty*, together with their encoded proteins, embody a reaction-diffusion circuit that works by local (short-range) activation and lateral (long-range) inhibition (Turing, 1952; Gierer and Meinhardt, 1972).

The establishment of a steady-state gradient of a diffusible morphogen generally requires a ‘sink’ that locally reduces the concentration of active morphogen (Crick, 1970). Recently it was shown that, in the formation of an FGF8 gradient in zebrafish embryos, this sink is provided by receptor-mediated endocytosis (Yu et al., 2009). Receptor-mediated endocytosis has long been known to regulate growth factor signaling (Sorkin and Waters, 1993), and has recently been implicated in controlling the strength of TGFβ signaling in

[2]Corresponding author: jcoffman@mdibl.org.
[1]These authors contributed equally to this work

vitro (Chen et al., 2009), but has not heretofore been shown to be involved in Nodal-mediated pattern formation.

In the sea urchin embryo, *nodal* is expressed on the presumptive oral (ventral) side of the blastula, which serves as an organizing center for specification of the secondary (oral-aboral) axis of the embryo and consequent patterning of both neuroectoderm (Duboc et al., 2004; Flowers et al., 2004; Yaguchi et al., 2007) and endomesoderm (Duboc et al., 2010). Nodal-dependent axis specification is perturbed by nickel chloride, exposure to which at late blastula stage causes *nodal* to become ectopically expressed in a radial pattern, throughout the circum-equatorial region that normally differentiates into oral and aboral ectoderm (Hardin et al., 1992; Duboc et al., 2004; Flowers et al., 2004; Agca et al., 2009). We show here that low micromolar zinc chloride has a similar radializing effect, which occurs via a progressive expansion of *nodal* expression beyond the confines of its initially localized domain in the prospective oral field. Cadmium on the other hand does not radialize embryos, but instead causes a general retardation of ectoderm differentiation. The differential effects of these divalent metals were exploited in an unbiased screen for genes that are similarly perturbed by nickel and zinc but not cadmium, using comparative deep RNA sequence analysis (RNAseq) (Mortazavi et al., 2008), with the objective of identifying cell physiological processes that regulate Nodal signaling. This analysis identified several genes associated with endocytosis, which led us to hypothesize that receptor-mediated endocytosis is required to localize the Nodal community effect. We tested the hypothesis using pharmacological inhibition of dynamin, a GTPase required for receptor-mediated endocytosis, and found that as predicted, this treatment phenocopied the radializing effects of nickel and zinc. These findings are the first reported indication that dynamin-mediated endocytosis functions as a sink to limit the range of Nodal signaling.

RESULTS

Nickel and zinc ions induce expansion of nodal expression after its initial localization

Embryos exposed to $NiCl_2$ from mid- to late blastula stage become radialized owing to development of oral ectoderm at the expense of aboral ectoderm (Hardin et al., 1992), an effect that is caused by a expanded domain of *nodal* expression around the entire equatorial circumference of the embryo (Duboc et al., 2004; Flowers et al., 2004). We found that exposure of *S. purpuratus* embryos to 1–2 μM $ZnCl_2$ from 12–24 hours post-fertilization (hpf) produces a similar radialized phenotype (Fig. 1A). The late window of vulnerability to both metals corresponds to the maintenance phase of *nodal* expression, after its zygotic activation (at ~6–7 hpf) and localization (by 12 hpf) to prospective oral ectoderm in *S. purpuratus* (Flowers et al., 2004; Nam et al., 2007). As previously reported for nickel in other species (Duboc et al., 2004), the ectopic expression of *nodal* induced by zinc is confined to the circum-equatorial region that gives rise to oral and aboral ectoderm, and is excluded from the vegetal plate and animal pole domains (Fig. 1A), which respectively give rise to endomesoderm and neuroectoderm. In contrast, nickel appears to induce ectopic expression in the animal pole domain as well (Fig. 1A), possibly reflecting interspecies differences in nickel sensitivity.

Following its initial activation at late cleavage stage, Nodal signaling amplifies and maintains *nodal* expression via a positive feedback community effect (Duboc et al., 2004; Bolouri and Davidson, 2010), which can be disrupted by pharmacological inhibition of the Alk4/5/7 receptor kinase that transduces the Nodal signal (Supp. Fig. S1 A, B). We found that development of oral-aboral (OA) polarity can be blocked even when the kinase inhibitor is applied at late-blastula stage (Supp. Fig. S1 C), indicating that OA axis specification requires the Nodal community effect to be active throughout blastula stage. The fact that exposure of embryos to nickel and zinc at mid-to late-blastula stage causes radialized *nodal*

expression (Fig. 1A) suggests that these metals perturb regulatory processes that confine the Nodal community effect to prospective oral ectoderm. Consistent with this, the addition of nickel or zinc chloride to embryo cultures beginning at mid-blastula stage (14 hpf) causes the expression of both *nodal* and *lefty* to spread progressively beyond the initially localized domain of expression (Fig. 1B; Supp. Fig. S2). Moreover, partial knockdown of *nodal* expression using a morpholino antisense oligonucleotide that blocks Nodal translation rescues an OA axis in nickel or zinc treated embryos (Supp. Fig. S3), demonstrating that *nodal* expression is required for the radializing effect of these metals. Together these data suggest that nickel and zinc ions abolish the boundary on the Nodal community effect that is normally maintained by Lefty, with the implication that these ions disrupt the physiological parameters required for Lefty-mediated inhibition.

Genes involved in endocytosis are perturbed by nickel and zinc but not cadmium

To obtain clues as to the mechanism underlying nickel- and zinc-induced expansion of Nodal signaling we performed SOLiD3 RNA sequencing (RNAseq) of total RNA isolated from late blastula stage (24hr) *S. purpuratus* embryos that were either untreated, or treated with nickel, zinc, or cadmium beginning at early blastula stage (10 hpf). Cadmium was chosen as a control because we had previously found cadmium was either ineffective (data not shown), or considerably less effective than nickel or zinc, as a radializing agent (Supp. Fig. S4). RNAseq analysis of the relative expression levels of representative marker genes for each embryonic territory showed that whereas both nickel and zinc specifically suppress expression of aboral ectoderm genes (consistent with the expansion of the Nodal community effect in these embryos), cadmium inhibits the expression of both oral and aboral ectoderm genes, as well as genes that mark the animal plate neuroectoderm (e.g., *six3, nkx2.1*) (Fig. 2). Moreover, the very early blastula (VEB) genes *SpAN* and *SpHE* [which are normally down-regulated by late blastula stage (Reynolds et al., 1992)] were significantly over-expressed in the cadmium-treated embryos, but not in the nickel- and zinc-treated embryos (Supp. Fig. S5), suggesting that cadmium causes a general retardation of development, whereas nickel and zinc do not. Finally, hierarchical clustering of the SOLiD3 data indicate that the gene expression profiles of nickel- and zinc-treated embryos are most similar to each other, and are more similar to untreated controls than to cadmium-treated embryos (Supp. Fig. S6). These data suggest that unlike nickel and zinc, which “oralize” ectoderm by inducing ectopic *nodal* expression, cadmium simply inhibits (or delays) ectoderm differentiation.

Comparison of the data from the SOLiD3 RNAseq analysis with data obtained from a previous Illumina GA RNAseq analysis of 24 hr zinc-treated versus untreated embryos revealed considerable variation between the results of the two experiments, with greater similarity between zinc-treated and untreated samples within each experiment than between untreated (or zinc-treated) samples from each experiment (Supp. Fig. S6). This proved to be a useful filter for identifying candidate genes and/or processes involved in Nodal regulation, because although a large number of genes were affected by zinc in each experiment, most of these were not consistently affected between experiments (probably reflecting biological variation between the two outbred cultures as well as differences in the sequencing platforms employed). An initial comparison of the results from the two experiments identified only 44 genes represented by an arbitrarily chosen expression threshold of at least 5 RPKM (representing a relatively low level of expression), that were consistently down-regulated ≥2.5-fold in response to zinc (Fig. 3A). For this subset of 44 genes, the SOLiD3 data were interrogated to ask which ones were similarly affected by nickel (8 genes) but not cadmium. Remarkably, of this group only two genes met this criterion, only one of which was clearly-identifiable (Fig. 3B): SCAMP1 (secretory carrier membrane protein 1), which has been implicated in the internalization of clathrin-coated pits during receptor-mediated

endocytosis (Fernandez-Chacon et al., 2000). When the screen was repeated with a wider filter (accepting genes represented by ≥2 RPKM, with ≥2-fold change), 59 genes were identified as being similarly affected by zinc (in both RNAseq experiments) and nickel but not cadmium, seven of which encoded proteins involved in vesicular trafficking and/or endocytosis (Table 1). Based on these findings we hypothesized that receptor-mediated endocytosis is required for *nodal*-mediated axis specification.

Dynamin activity is required to restrict the domain of Nodal signaling

Receptor-mediated endocytosis requires the activity of the protein dynamin, a GTPase that participates in the scission process that internalizes coated vesicles containing the receptor-ligand complex (Ungewickell and Hinrichsen, 2007). The sea urchin genome encodes two classical dynamins (Beane et al., 2006), one of which was recently cloned and shown to be expressed in oocytes and to mediate endocytosis therein (Brooks and Wessel, 2004). Dynasore is a specific pharmacological inhibitor of dynamin (Macia et al., 2006) shown recently to augment TGFβ signaling *in vitro* by inhibiting clathrin-dependent endocytosis (Chen et al., 2009). As predicted by our hypothesis, blastula stage embryos treated with relatively low concentrations of Dynasore (6–12 μM, below the reported IC50 value of 15 μM; Macia et al. 2006) became radialized, closely phenocopying embryos exposed to nickel or zinc (or embryos that over-express *nodal*; Fig. 4A). Whole mount in situ hybridization (WMISH) was performed to ascertain whether this phenotype is caused by radialized expression of *nodal*. In mesenchyme blastula stage embryos treated with Dynasore, *nodal* was expressed in a circum-equatorial pattern identical to that observed in nickel and zinc-treated embryos, both when the treatment was initiated at mid-blastula stage (Fig 4A, panel 5), following the localization of *nodal* expression to prospective oral ectoderm, and at late cleavage stage (Fig. 4A, panel 6), the time at which *nodal* is zygotically activated. These results indicate that dynamin activity is required for both establishing and maintaining a localized domain of *nodal* expression within the embryonic ectoderm, suggesting that axis specification via *nodal* and *lefty* requires dynamin-mediated endocytosis.

DISCUSSION

That axis specification via the Nodal/Lefty feedback circuit is controlled by dynamin is consistent with previous proposals that Nodal signaling drives pattern formation by way of short-range activation and long-range inhibition (Juan and Hamada, 2001; Solnica-Krezel, 2003). In this case the inhibition is executed by Lefty, which is more diffusible than Nodal and competitively interferes with the ability of the latter to activate its receptor (Sakuma et al., 2002; Chen and Shen, 2004; Cheng et al., 2004). Although it has not yet been directly demonstrated in the sea urchin embryo, this greater range of diffusion is presumably the mechanism through which Lefty confines the *nodal* community effect to prospective oral ectoderm (Duboc et al., 2004; Duboc et al., 2008; Bolouri and Davidson, 2010). Recently it was reported that the extracellular diffusion of Nodal is restricted by sulfated glycosaminoglycans (Bergeron et al., in press). It has also been shown that the mature (proteolytically processed) Nodal protein is unstable and rapidly turned over via endocytosis, which significantly limits its range (Le Good et al., 2005). Since Lefty-mediated lateral inhibition is sensitive to stoichiometry, increasing either the diffusibility or the stability of Nodal might be expected to expand the community effect. Our results are consistent with the proposition that dynamin-mediated endocytosis promotes the decay of the Nodal ligand, providing a ‘sink’ that limits its range of signaling, thus allowing Lefty to function as a long-range inhibitor.

While in retrospect it might have been deduced *a priori* from the above considerations, our hypothesis that dynamin-mediated endocytosis controls *nodal*-mediated pattern formation was in fact generated by an unbiased gene expression screen that took advantage of inter-

and intra-experimental variation in the response to metal-induced perturbations of Nodal regulation. This allowed us to filter out the many genes that responded variably to zinc treatment in different experiments, and thus identify a small subset that was consistently affected (Fig. 3A). Further filtering took advantage of the fact that nickel and zinc produce a similar teratogenic effect via *nodal* (Figs. 1 and 2) that is not recapitulated by cadmium, which allowed us to eliminate genes that are non-specifically affected by exposure to divalent metal ions, as well as any genes that are specifically affected by nickel or zinc but not both. Among the very small subset of genes identified as being both consistently and strongly down-regulated by zinc and nickel but not cadmium, several encoded proteins that play a role in endocytosis and/or vesicular trafficking (Fig. 3B and Table 1). Included in this group was the sea urchin homolog of SCAMP1, a protein that is thought to participate in the endocytosis of clathrin-coated pits (Fernandez-Chacon et al., 2000). This led us to hypothesize that endocytosis is required to limit the range of Nodal signaling, which we tested by inhibiting dynamin, a GTPase essential for clathrin-mediated endocytosis (Macia et al., 2006). Toward that end we used Dynasore, a drug that was recently shown to enhance the strength of TGFβ signaling by inhibiting clathrin-dependent endocytosis (Chen et al., 2009). As predicted, Dynasore treatment closely phenocopied the teratogenic effects of nickel and zinc, providing strong initial support for our hypothesis. Although the simplest explanation of these results involves direct endocytosis of Nodal protein, further work is needed to confirm this. It will also be important to determine how our results relate to those of Blanchet et al. (2008) showing that Nodal-Cripto signal transduction complexes localize via clathrin-independent endocytosis to early endosomes, since Dynasore does not appear to interfere with Nodal signaling.

The hypothesis that nickel and zinc ions radialize *nodal* expression by interfering with endocytosis is reasonable since zinc has been shown to inhibit receptor-mediated endocytosis *in vitro* (McAbee and Jiang, 1999). Moreover, both zinc and nickel are calcium-channel inhibitors (Nikonenko et al., 2005), and hence might be expected to interfere with calcium signaling, which is required for dynamin-mediated endocytosis (Lai et al., 1999; Maria Cabeza et al., 2010; Sakai et al., 2010). For the purposes of this study nickel and zinc were simply tools for identifying candidate processes involved in the regulation of Nodal feedback control, which is perturbed by those metals (Fig. 1). How nickel and zinc affect endocytosis and the expression of genes involved in that process remain open questions. It is clear however that in embryos undergoing *nodal*-mediated epigenesis, environmental exposures that inhibit dynamin-mediated endocytosis are likely to be teratogenic.

EXPERIMENTAL PROCEDURES

Gamete procurement and embryo culture

Adult *Strongylocentrotus purpuratus* were obtained from the Pt. Loma Marine Invertebrate Lab (Lakeside, CA). Standard procedures were used to obtain gametes, fertilize eggs, microinject, and culture embryos. For experiments using pre-hatching blastulae, eggs were fertilized in 1 mM para-aminobenzoic acid (PABA) in filtered seawater (FSW).

For the WMISH time-course (Supp. Fig. S2), aliquots of embryos exposed to 2 μM $ZnCl_2$ or 15 μM $NiCl_2$ beginning at 14 were collected at regular intervals up to 20 hrs. For unhatched blastulae, the fertilization envelope was removed by passing embryos through a BD-Falcon 70μm nylon cell strainer. The embryos were fixed in 4% paraformaldehyde in FSW with 20 mM EPPS (Sigma E1894) pH 8.0 for 1 hr. After washing twice in PBS with 0.1% Tween (PBST), they were treated with proteinase K (5 μg/ml in PBST) for 2 min. Embryos were washed 3 times in −20°C methanol and stored at −20°C until assayed. An aliquot of each batch of treated embryos was developed for 48–72 hrs to assure that the embryos developed the radicalized phenotype.

For RNAseq experiments, $NiCl_2$ (15 μM), $ZnCl_2$ (1 μM), or $CdCl_2$ (10 μM) were added to cultures at 10 hpf, and the embryos were harvested by centrifugation at 24 hpf and frozen at −80°C. An aliquot of each culture was developed to 72 hpf to assess the effects of the treatments on secondary axis development (Supp. Fig. S4).

To inhibit dynamin, Dynasore (6–12μM) was added to embryo cultures at either 6 hpf (32 cell stage), the stage at which *nodal* is initially activated, or 12 hpf (early blastula), a stage at which *nodal* expression is clearly localized to the prospective oral field.

To partially knock down Nodal (Supp. Fig. S3), 2–5 pl of 120 mM KCl solution, containing a morpholino antisense oligonucleotide (at 50 μM) that targets the sequence immediately upstream of the Nodal translation start site, was injected into zygotes. The sequence of the MASO was 5′-TGCATGGTTAAAAGTCCTTAAAAAT-3′.

Whole Mount In Situ Hybridization (WMISH)

Gene expression was visualized using digoxigenin and fluorescein labeled antisense riboprobes to *nodal*, *lefty*, or *foxQ2*. Embryos were rehydrated at room temp (RT) in PBS (all WMISH buffers contained 0.1 % Tween-20) followed by a wash in hybridization buffer (HB) containing 50% formamide, 5x Denhardts, 5x SSC, 1 mg/ml yeast RNA, and 50 μg/ml heparin. Embryos were incubated in fresh HB for 1 hour (65°C), then probed overnight (65°C) in HB with 2 ng/μl of a probe at least 390 bp and that spanned at least one intron. The embryos were next washed with a series of buffers at 60°C starting with fresh HB, 50% HB with 2x SSC and 2x SSC for 15 min each, then 0.2x SSC and 0.1x SSC for 20 min each. This was followed by 3 washes at RT with 0.1M Maelic Acid pH 7.2 and 0.15M NaCl (filter-sterilized; MAB). Embryos were blocked for 30 min at room temp in MAB containing 1% Roche Block (cat no. 11 096 176 001) and 5% goat serum (MABBG). Embryos were incubated with the appropriate anti-fluoroscein or anti-digoxygenin antibody conjugate to horseradish peroxidase (Roche) at 1.5 units/ml in MABBG for 1 hr at RT. After 3 × 15 min washes in PBS, the PerkinElmer substrate (8:400 diluent) was incubated for 30 min (TSA-Plus Kit NEL753) in the dark, and then washed 4 × 5 min in PBS at RT.

In dual label WMISH experiments the same procedure was followed except the buffer contained 2 probes, each with a different label. After staining with an antibody against one label as outlined, the peroxidase activity was quenched with 0.15 % H_2O_2 in PBS followed by a 5 min wash in PBS and 3 × 5 min washes in MAB. The second antibody for the opposite label (fluorescein or digoxygenin) was incubated as above and stained with the Perkin Elmer kit. The Cy3-Tyramide was always the first substrate as the fluorescein was quenched by the H_2O_2. Embryos were washed 4 × 5 min in PBS at RT and stored at 5°C until visualized with a Zeiss Meta 510 Confocal microscope.

Deep RNA Sequencing (RNASeq)

Total RNA was purified using an RNAaqueous midi-kit (Ambion), from approximately 100,000 mesenchyme blastula stage (24) *S. purpuratus* embryos that were either untreated, or treated with $ZnCl_2$, $NiCl_2$, or $CdCl_2$. For one experiment (untreated vs. zinc-treated) the RNA was subjected to Illumina Genome Analyzer RNAseq analysis at the DNA Sequencing Center of the Cornell University Life Sciences Core Laboratories Center (Ithaca, NY, USA). For a second experiment (using a different culture of untreated, zinc-treated, nickel-treated, and cadmium-treated embryos) the RNA was subjected to SOLiD3 RNAseq analysis at the Molecular Genetics Core Facility of the Children's Hospital Boston and Harvard University (Boston MA, USA).

The sequence reads from both RNAseq experiments were imported into the CLC bio Genomics Workbench (GW) along with build 2.1 of the *S. purpuratus* reference genome in

Genbank format. The reads were mapped to the reference genome using RNA-seq Analysis in GW, which maps each read to the genome and counts only those that uniquely map to an annotated exon or UTR region. The gene counts were normalized as reads per kilobase of exon model per million mapped reads (RPKM) (Mortazavi et al., 2008).

The data table containing all of the RPKM values was filtered by the ratio of metal-treated RPKM to untreated RPKM for each gene, which was used to rank the fold-differences in expression between treated and untreated samples in each culture. This ranking was then used at specified thresholds to identify (1) genes that were consistently inhibited by zinc in two separate experiments, and from that subset, (2) genes that were similarly affected by nickel but not cadmium in the second experiment.

Supplementary Material

Refer to Web version on PubMed Central for supplementary material.

Acknowledgments

This work was funded by the NIH (R01-ES016722 and P30-ES003828). DS was supported by an NSF REU fellowship (DBI 0453391). We thank Peter Knowlton for assisting with the SB431542 time-course experiments.

References

Agca C, Klein WH, Venuti JM. Respecification of ectoderm and altered Nodal expression in sea urchin embryos after cobalt and nickel treatment. Mech Dev. 2009; 126:430–442. [PubMed: 19368800]

Beane WS, Voronina E, Wessel GM, McClay DR. Lineage-specific expansions provide genomic complexity among sea urchin GTPases. Dev Biol. 2006; 300:165–179. [PubMed: 17014838]

Bergeron KF, Xu X, Brandhorst BP. Oral-aboral patterning and gastrulation of sea urchin embryos depend on sulfated glycosaminoglycans. Mech Dev. In press.

Blanchet MH, Le Good JA, Oorschot V, Baflast S, Minchiotti G, Klumperman J, Constam DB. Cripto localizes Nodal at the limiting membrane of early endosomes. Sci Signal. 2008; 1:ra13. [PubMed: 19001664]

Bolouri H, Davidson EH. The gene regulatory network basis of the “community effect,” and analysis of a sea urchin embryo example. Dev Biol. 2010; 340:170–178. [PubMed: 19523466]

Brooks JM, Wessel GM. The major yolk protein of sea urchins is endocytosed by a dynamin-dependent mechanism. Biol Reprod. 2004; 71:705–713. [PubMed: 15084478]

Chea HK, Wright CV, Swalla BJ. Nodal signaling and the evolution of deuterostome gastrulation. Dev Dyn. 2005; 234:269–278. [PubMed: 16127715]

Chen C, Shen MM. Two modes by which Lefty proteins inhibit nodal signaling. Curr Biol. 2004; 14:618–624. [PubMed: 15062104]

Chen CL, Hou WH, Liu IH, Hsiao G, Huang SS, Huang JS. Inhibitors of clathrin-dependent endocytosis enhance TGFbeta signaling and responses. J Cell Sci. 2009; 122:1863–1871. [PubMed: 19461075]

Chen Y, Schier AF. Lefty proteins are long-range inhibitors of squint-mediated nodal signaling. Curr Biol. 2002; 12:2124–2128. [PubMed: 12498687]

Cheng SK, Olale F, Brivanlou AH, Schier AF. Lefty blocks a subset of TGFbeta signals by antagonizing EGF-CFC coreceptors. PLoS Biol. 2004; 2:E30. [PubMed: 14966532]

Crick F. Diffusion in embryogenesis. Nature. 1970; 225:420–422. [PubMed: 5411117]

Duboc V, Lapraz F, Besnardeau L, Lepage T. Lefty acts as an essential modulator of Nodal activity during sea urchin oral-aboral axis formation. Dev Biol. 2008; 320:49–59. [PubMed: 18582858]

Duboc V, Lapraz F, Saudemont A, Bessodes N, Mekpoh F, Haillot E, Quirin M, Lepage T. Nodal and BMP2/4 pattern the mesoderm and endoderm during development of the sea urchin embryo. Development. 2010; 137:223–235. [PubMed: 20040489]

Duboc V, Rottinger E, Besnardeau L, Lepage T. Nodal and BMP2/4 signaling organizes the oral-aboral axis of the sea urchin embryo. Dev Cell. 2004; 6:397–410. [PubMed: 15030762]

Duboc V, Rottinger E, Lapraz F, Besnardeau L, Lepage T. Left-right asymmetry in the sea urchin embryo is regulated by nodal signaling on the right side. Dev Cell. 2005; 9:147–158. [PubMed: 15992548]

Fernandez-Chacon R, Achiriloaie M, Janz R, Albanesi JP, Sudhof TC. SCAMP1 function in endocytosis. J Biol Chem. 2000; 275:12752–12756. [PubMed: 10777571]

Flowers VL, Courteau GR, Poustka AJ, Weng W, Venuti JM. Nodal/activin signaling establishes oral-aboral polarity in the early sea urchin embryo. Dev Dyn. 2004; 231:727–740. [PubMed: 15517584]

Gierer A, Meinhardt H. A theory of biological pattern formation. Kybernetik. 1972; 12:30–39. [PubMed: 4663624]

Grande C, Patel NH. Nodal signalling is involved in left-right asymmetry in snails. Nature. 2009; 457:1007–1011. [PubMed: 19098895]

Hardin J, Coffman JA, Black SD, McClay DR. Commitment along the dorsoventral axis of the sea urchin embryo is altered in response to NiCl2. Development. 1992; 116:671–685. [PubMed: 1289059]

Juan H, Hamada H. Roles of nodal-lefty regulatory loops in embryonic patterning of vertebrates. Genes Cells. 2001; 6:923–930. [PubMed: 11733030]

Lai MM, Hong JJ, Ruggiero AM, Burnett PE, Slepnev VI, De Camilli P, Snyder SH. The calcineurin-dynamin 1 complex as a calcium sensor for synaptic vesicle endocytosis. J Biol Chem. 1999; 274:25963–25966. [PubMed: 10473536]

Le Good JA, Joubin K, Giraldez AJ, Ben-Haim N, Beck S, Chen Y, Schier AF, Constam DB. Nodal stability determines signaling range. Curr Biol. 2005; 15:31–36. [PubMed: 15649361]

Lupo G, Harris WA, Lewis KE. Mechanisms of ventral patterning in the vertebrate nervous system. Nat Rev Neurosci. 2006; 7:103–114. [PubMed: 16429120]

Macia E, Ehrlich M, Massol R, Boucrot E, Brunner C, Kirchhausen T. Dynasore, a cell-permeable inhibitor of dynamin. Dev Cell. 2006; 10:839–850. [PubMed: 16740485]

Maria Cabeza J, Acosta J, Ales E. Dynamics and regulation of endocytotic fission pores: role of calcium and dynamin. Traffic. 2010; 11:1579–1590. [PubMed: 20840456]

McAbee DD, Jiang X. Copper and zinc ions differentially block asialoglycoprotein receptor-mediated endocytosis in isolated rat hepatocytes. J Biol Chem. 1999; 274:14750–14758. [PubMed: 10329671]

Mortazavi A, Williams BA, McCue K, Schaeffer L, Wold B. Mapping and quantifying mammalian transcriptomes by RNA-Seq. Nat Methods. 2008; 5:621–628. [PubMed: 18516045]

Nam J, Su Y-H, Lee PY, Robertson AJ, Coffman JA, Davidson EH. Cis-regulatory control of the nodal gene, initiator of the sea urchin oral ectoderm gene network. Dev Biol. 2007; 306:860–869. [PubMed: 17451671]

Nikonenko I, Bancila M, Bloc A, Muller D, Bijlenga P. Inhibition of T-type calcium channels protects neurons from delayed ischemia-induced damage. Mol Pharmacol. 2005; 68:84–89. [PubMed: 15851654]

Range R, Lapraz F, Quirin M, Marro S, Besnardeau L, Lepage T. Cis-regulatory analysis of nodal and maternal control of dorsal-ventral axis formation by Univin, a TGF-{beta} related to Vg1. Development. 2007; 134:3649–3664. [PubMed: 17855430]

Reynolds SD, Angerer LM, Palis J, Nasir A, Angerer RC. Early mRNAs, spatially restricted along the animal-vegetal axis of sea urchin embryos, include one encoding a protein related to tolloid and BMP-1. Development. 1992; 114:769–786. [PubMed: 1618141]

Sakai H, Moriura Y, Notomi T, Kawawaki J, Ohnishi K, Kuno M. Phospholipase C-dependent Ca2+-sensing pathways leading to endocytosis and inhibition of the plasma membrane vacuolar H+-ATPase in osteoclasts. Am J Physiol Cell Physiol. 2010; 299:C570–578. [PubMed: 20592242]

Sakuma R, Ohnishi Yi Y, Meno C, Fujii H, Juan H, Takeuchi J, Ogura T, Li E, Miyazono K, Hamada H. Inhibition of Nodal signalling by Lefty mediated through interaction with common receptors and efficient diffusion. Genes Cells. 2002; 7:401–412. [PubMed: 11952836]

Schier AF, Shen MM. Nodal signalling in vertebrate development. Nature. 2000; 403:385–389. [PubMed: 10667782]

Shen MM. Nodal signaling: developmental roles and regulation. Development. 2007; 134:1023–1034. [PubMed: 17287255]

Solnica-Krezel L. Vertebrate development: taming the nodal waves. Curr Biol. 2003; 13:R7–9. [PubMed: 12526755]

Sorkin A, Waters CM. Endocytosis of growth factor receptors. Bioessays. 1993; 15:375–382. [PubMed: 8395172]

Su YH, Li E, Geiss GK, Longabaugh WJ, Kramer A, Davidson EH. A perturbation model of the gene regulatory network for oral and aboral ectoderm specification in the sea urchin embryo. Dev Biol. 2009; 329:410–421. [PubMed: 19268450]

Turing AM. The chemical basis of morphogenesis. Bull Math Biol. 1952; 52:153–197. [PubMed: 2185858]

Ungewickell EJ, Hinrichsen L. Endocytosis: clathrin-mediated membrane budding. Curr Opin Cell Biol. 2007; 19:417–425. [PubMed: 17631994]

Yaguchi S, Yaguchi J, Angerer RC, Angerer LM. A Wnt-FoxQ2-nodal pathway links primary and secondary axis specification in sea urchin embryos. Dev Cell. 2008; 14:97–107. [PubMed: 18194656]

Yaguchi S, Yaguchi J, Burke RD. Sp-Smad2/3 mediates patterning of neurogenic ectoderm by nodal in the sea urchin embryo. Dev Biol. 2007; 302:494–503. [PubMed: 17101124]

Yu SR, Burkhardt M, Nowak M, Ries J, Petrasek Z, Scholpp S, Schwille P, Brand M. Fgf8 morphogen gradient forms by a source-sink mechanism with freely diffusing molecules. Nature. 2009; 461:533–536. [PubMed: 19741606]

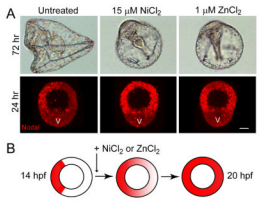

Figure 1.

Transient exposure of blastula stage embryos to low micromolar nickel and zinc ions causes radialized development owing to ectopic *nodal* expression. (A) Phenotypes of untreated, nickel-treated, and zinc-treated embryos at 72 hrs post-fertilization (hpf) showing morphology of early larvae, and at 24 hpf showing the expression domain of *nodal* assayed by fluorescent whole-mount in situ hybridization. The embryos are all oriented with the vegetal plate (V) at the bottom of the frame. Note that in the nickel-treated embryo the domain of *nodal* expression appears to expand into the apical plate. Bar = 20 μm. (B) Summary diagram depicting the progressive expansion of the expression domain of *nodal* and *lefty* (whose mRNAs are co-localized) following addition of nickel or zinc to the culture medium at mid-blastula stage (data shown in Supp. Fig. S2). The circles represent equatorial cross-sections of embryos bisecting the animal-vegetal axis.

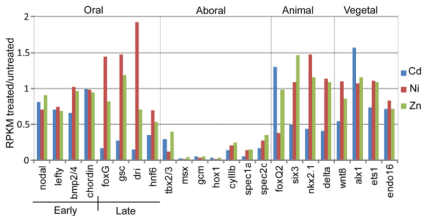

Figure 2.

Relative expression levels (RPKM treated/RPKM untreated for each treatment) of territory-specific genes in nickel-treated, zinc-treated, and cadmium-treated embryos measured by SOLiD3 RNAseq. The territories are: oral ectoderm, aboral ectoderm (or mesoderm in the case of *gcm*), animal plate neuroectoderm, and vegetal plate endomesoderm. The early oral genes are activated at late cleavage to early blastula stage (6–9 hpf), prior to the time at which the metals were added to the culture medium (12 hpf), whereas the late oral genes are normally activated after this time, in response to the nuclear regulatory state established by the Nodal community effect (Su et al., 2009; Bolouri and Davidson, 2010).

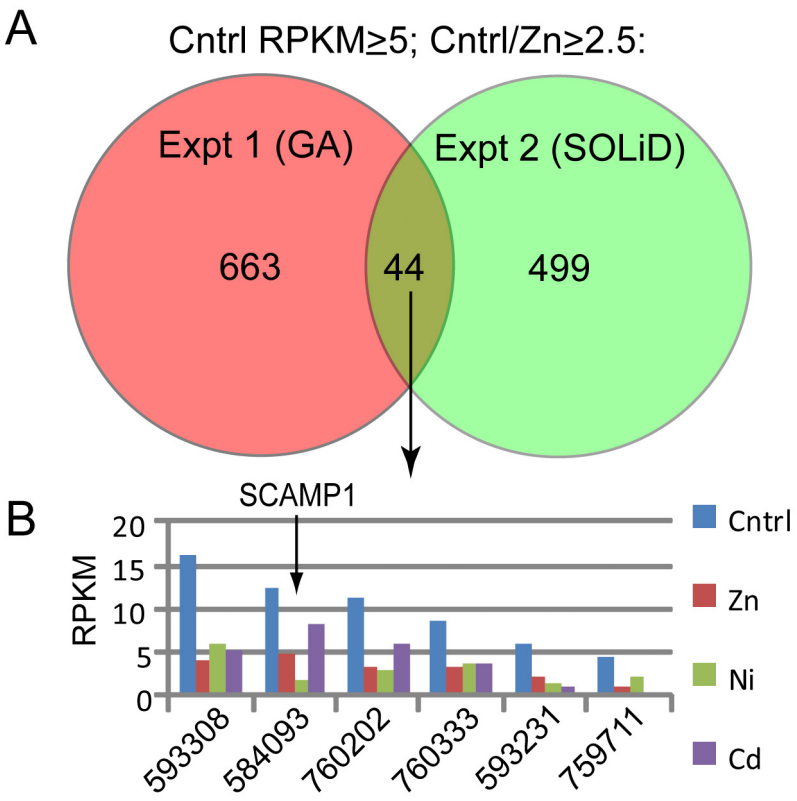

Figure 3.

Identification of genes affected by nickel and zinc but not cadmium. (A) Venn diagram of comparing results of two RNAseq experiments measuring gene expression in untreated and zinc-treated embryos at 24 hpf, showing numbers of genes displaying ≥5 RPKM in the untreated embryos that were underexpressed ≥2.5 fold in the zinc-treated embryos. (B) Graph showing expression levels of six of the eight loci from the common set shown in (A) that were identified in the SOLiD3 dataset as having a ≥2.5 fold reduction in expression in response to nickel.

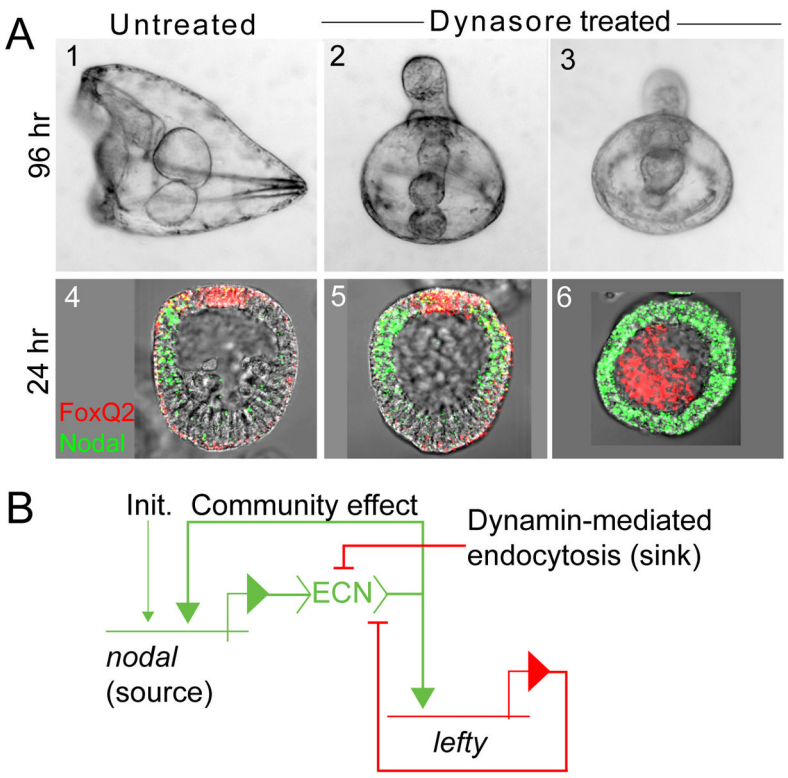

Figure 4.

Inhibition of dynamin-mediated endocytosis radializes embryos by causing ectopic *nodal* expression. (A) Phenotypes of untreated (panels 1 and 4) and Dynasore-treated (panels 2, 3, 5 and 6) embryos, showing larval phenotype at 96 hpf (panels 1–3), and *nodal* expression pattern at mesenchyme blastula stage (24 hpf, WMISH; panels 4–6). Expression of *foxQ2* (red), a negative regulator of *nodal* (Yaguchi et al., 2008), marks the animal pole ectoderm and is used for orientation. The embryos in panels 2, 3 and 5 were treated with 12 μM Dynasore from 12 hpf on; the embryo in panel 6 was treated with 6 μM Dynasore from 6 hpf on, the time at which *nodal* is zygotically activated. (B) Updated model of the controlled feedback circuit underlying *nodal*-mediated epigenesis. “Init” = the initial (*nodal*-independent) activator of *nodal*, which is pan-ectodermal (Nam et al., 2007; Range et al., 2007); “ECN”= extracellular Nodal.

Table 1

Genes involved in vesicular trafficking represented by ≥2 RPKM, whose expression was reduced ≥2-fold by nickel and zinc but not cadmium

			RPKM treatment/RPKM control			
			Expt. 1 (GA)	Expt. 2 (SOLiD3)		
NCBI LOC#	Closest *Hs* homolog	Location and/or function	Zn	Zn	Ni	Cd
575087	CHMP1a	Endosome sorting	0.48	0.39	0.40	0.63
577394	SPTBN4	Membrane cytoskeleton, vesicles	0.40	0.20	0.30	0.87
583247	COG8	Golgi, membrane trafficking	0.50	0.41	0.36	0.60
584093	SCAMP1	Exo/endocytosis	0.32	0.38	0.16	0.65
584543	PDCD6IP	Endocytosis, apoptosis	0.39	0.40	0.38	0.52
591917	SYS1	Targeting to Golgi	0.37	0.41	0.43	0.83
766287	HOOK1	Cytoskeleton, endocytosis	0.37	0.24	0.12	1.04